Tethering of Nicotinamide Adenine Dinucleotide Inside Hollow Nanofibers for High-Yield Synthesis of Methanol from Carbon Dioxide Catalyzed by Coencapsulated Multienzymes

Xiaoyuan Ji,[†] Zhiguo Su,[†] Ping Wang,[†,‡] Guanghui Ma,[†] and Songping Zhang*[,†]

[†]National Key Laboratory of Biochemical Engineering, Institute of Process Engineering, Chinese Academy of Sciences, Beijing 100190, China and [‡]Department of Bioproducts and Biosystems Engineering and Biotechnology Institute, University of Minnesota, St. Paul, Minnesota 55108, United States

ABSTRACT Enzymatic conversion of carbon dioxide (CO_2) to fuel or chemicals is appealing, but is limited by lack of efficient technology for regeneration and reuse of expensive cofactors. Here we show that cationic polyelectrolyte-doped hollow nanofibers, which can be fabricated *via* a facile coaxial electrospinning technology, provide an ideal scaffold for assembly of cofactor and multienzymes capable of synthesizing methanol from CO_2 through a cascade multistep reaction involving cofactor regeneration. Cofactor and four enzymes including formate, formaldehyde, alcohol, and glutamate dehydrogenases were *in situ* coencapsulated inside the lumen of hollow nanofibers by involving them in the core-phase solution for coaxial electrospinning, in which cationic polyelectrolyte was predissolved. The polyelectrolyte penetrating across the shell of the hollow nanofibers enabled efficient tethering and retention of cofactor inside the lumen *via* ion-exchange interactions between oppositely charged polyelectrolytes and cofactor. With carbonic anhydrase assembled on the outer surface of the hollow nanofibers for accelerating hydration of CO_2, these five-enzymes-cofactor catalyst system exhibited high activity for methanol synthesis. Compared with methanol yield of only 36.17% using free enzymes and cofactor, the hollow nanofiber-supported system afforded a high value up to 103.2%, the highest reported value so far. It was believed that the linear polyelectrolytes acted as spacers to enhance the shuttling of cofactor between enzymes that were coencapsulated within near vicinity, thus improving the efficiency of the system. The immobilized system showed good stability in reusing. About 80% of its original productivity was retained after 10 reusing cycles, with a cofactor-based cumulative methanol yield reached 940.5%.

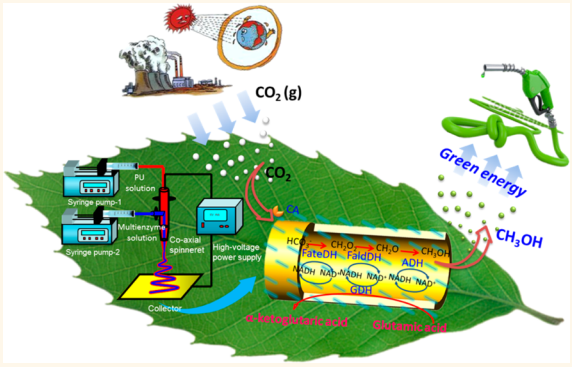

KEYWORDS: carbon dioxide · bioconversion · cofactor regeneration · hollow nanofibers · multienzyme system

Because of increasing concerns on global warming and energy crisis, efficient conversion of CO_2 to value added chemicals and fuels has been recognized as a promising strategy for mitigation of CO_2 related greenhouse gas effects.[1−4] Compared with electrochemical conversion[5−10] and photochemical conversion,[5,11−14] enzymatic conversion[1,15−20] is more attractive because of its intrinsic advantages like high efficiency, excellent selectivity, and mild reaction conditions.[3,21−23] One of the most popular biocatalytic routes is a cascade reduction approach, through which CO_2 is converted to methanol catalyzed by three different dehydrogenases, namely, formate dehydrogenase (FateDH), formaldehyde dehydrogenase (FaldDH), and alcohol dehydrogenase (ADH).[1,16,17] In this process, FateDH converts CO_2 to formate, which can then be reduced to formaldehyde by FaldDH, and finally formaldehyde is reduced to methanol by ADH.[1,16,17] To produce 1 mol of methanol through this cascade reduction reaction, 3 mol of reduced nicotinamide adenine dinucleotide (NADH) are stoichiometrically consumed, by acting as a terminal electron donor of each step of the reduction reaction.

* Address correspondence to spzhang@ipe.ac.cn.

Received for review February 27, 2015 and accepted April 10, 2015.

Published online April 10, 2015
10.1021/acsnano.5b01278

While the enzymatic synthesis of methanol from CO_2 is appealing, efficient regeneration and reusing of the cofactor are critical due to its high cost. In one of the earliest attempt to enzymatically converting CO_2 to methanol, three dehydrogenases were coimmobilized in silica sol−gel matrices.[1] With NADH added in free formation, the methanol yield based on NADH was only 43.8%. Sever activity loss of enzymes caused by toxic cosolvent and catalysts used for sol−gel encapsulation process was considered as the major reason for such low yield. A relatively mild biomimetic mineralization technology was developed recently to construct a microcapsule-based multienzyme cascade system for CO_2 conversion, with which the methanol yield was improved to 71.6%.[17] Nevertheless, construction of the microcapsule was so complicated, and immobilization and regeneration of expensive coenzyme were still undealt with.

For continuous bioprocess operation of cofactor-dependent enzymatic reactions, the challenging for cofactor regeneration and recycling is always associated with the retention of both enzymes and the small molecular cofactor in bioreactors. Immobilizing cofactor to solid materials, unfortunately, usually leads to inactive cofactors, since binding of cofactor to the active site of enzymes for electron/hydride transfer and cofactor regeneration will then be greatly hindered. One exception was based on utilization of nanoparticles, which were believed to bring the cofactor into contact with enzymes due to the collision between particles.[24] Several multienzyme systems involving cofactor regeneration had been realized by covalently binding enzymes and cofactors to outer surface of nanoparticles.[16,25,26] When the nanoparticle-based multienzymes and cofactor were tested for methanol synthesis from CO_2 and cofactor regeneration, however, the methanol yield was as low as less than 5%, significantly lower than that of the free enzyme system. Moreover, the operation and recycling of nanoparticles is a difficult task. Recently, DNA was used as scaffolds to create a multienzyme complex, in which an artificial swinging arm facilitates hydride transfer between two coupled dehydrogenases.[27] Although these methods were proven successfully to some extent, the efficient regeneration and reuse of the cofactor still remains as one of the biggest challenges in biology and material sciences.

As an alternative method, a facile coaxial electrospinning technology was adopted by us to prepare novel polyurethane (PU) hollow nanofibers. By simply involving the enzymes and cofactor in the core phase solution for coaxial electrospinning, a coupling bienzyme system for bile acid assay involving cofactor regeneration was *in situ* coencapsulated inside the lumen side of the hollow nanofibers.[28] Two dehydrogenases performing the coupling reaction were proven efficiently retained inside the lumen side of the hollow nanofiber by PU shell, which showed a characteristic molecular weight cutoff (MWCO) at approximately 20 kDa.[28] In contrast, the coencapsulated cofactor would release into solution immediately once immersing the hollow nanofiber membrane to buffer solution due to its small molecular weight; therefore, the recycling of cofactor was still unrealized. Inspired by the technology of layer-by-layer assembly, a PU hollow nanofiber doped with cationic polyelectrolyte was later fabricated and used as a novel scaffold supporting positional assembly of a bienzyme system, one enzyme was *in situ* encapsulated inside the lumen side of the hollow nanofibers, while the other one was assembled on the outer surface *via* ion-exchange interactions between oppositely charged enzymes and polyelectrolyte.[29]

Since the linear polyelectrolyte is penetrated across the shell of the hollow nanofiber, the polyelectrolyte-doped hollow nanofiber is expected not only to serve as a scaffold for assembling of multienzymes, the polyelectrolyte may also provide binding site for possible specific tethering of the cofactors, which is also negatively charged. By simply adding cofactors and enzymes along with polyelectrolytes to the core-phase solution for coaxial electrospinning, a hollow nanofiber-based catalytic system will be fabricated. At the same time, the polyelectrolyte is expected to act as spacers for the tethered cofactor, allowing more efficient shuttling of the cofactors between different enzymes within the near vicinity inside the lumen side of the hollow nanofibers. With the formation of nonwoven membrane, such catalytic systems are easily operated and recycled.

To test the feasibility and advantages of the proposed hollow nanofibers based cofactor-enzyme catalyst, the multienzyme system for cascade reduction of CO_2 to methanol involving FateDH, FaldDH, ADH, and NADH were *in situ* coencapsulated in the lumen inside of the polyelectrolyte-doped hollow nanofibers. Glutamate dehydrogenase (GDH) was also introduced into the lumen side for continuous regeneration of the cofactor. Moreover, to accelerate the hydration of CO_2, carbonic anhydrase (CA) was assembled on the outer surface of the hollow nanofibers.

RESULTS AND DISCUSSION

Fabrication and Characterization of Polyelectrolyte Doped Hollow Nanofibers. In one of our recent work, a facile coaxial electrospinning technique have been successfully developed to prepare a hollow PU nanofibers, whose shell showed a MWCO about 20 kDa, thus enabled efficient *in situ* encapsulation enzymes with molecular weight above 20 kDa inside the lumen of the hollow nanofibers.[28] Here in the present work, to accomplish retention of NADH, which has molecular weight only 663 Da, inside the lumen of hollow nanofibers, a water-soluble cationic polyelectrolyte, poly(allylamine

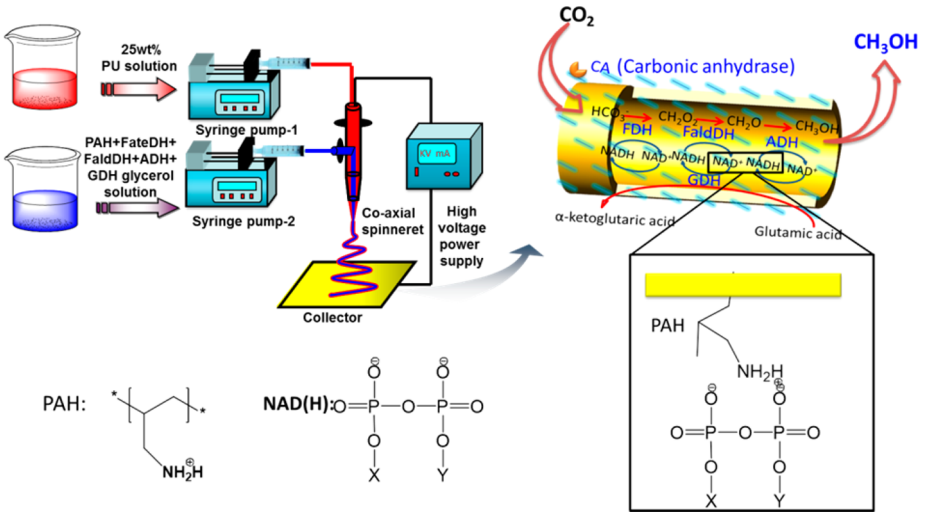

Scheme 1. Schematic illustration of the setup for coaxial electrospinning for constructing hollow nanofiber-supported multienzyme system for methanol synthesis from CO_2 with *in situ* regeneration of NADH.

hydrochloride) (PAH), was doped in the PU nanofibers by simply dissolving it in the core-phase solution for coaxial electrospinning (Scheme 1). It was expected the electrostatic interactions between ionizable groups of PAH and negatively charged NADH will enable tethering of coenzyme molecule tightly onto the inner surface of the shell of hollow nanofibers, thus facilitating its immobilization and shuttling between coencapsulated oxidoreductases for more efficient regeneration of NAD(H).

To verify the feasibility of electrostatic interactions assisted retention of NADH inside the lumen of hollow nanofibers, hollow nanofibers doped with different amount of PAH were prepared by involving 10 mg/mL NADH and different amount of PAH (concentration ranges from 0 to 30 mg/mL) in the core-phase solution for coaxial electrospinning. Figure 1 shows the SEM images of the as-electrospun hollow nanofibers with *in situ* immobilized NADH at different PAH concentration. Averagely, when the concentration of PAH in core-phase solution was increased from 0 to 10 mg/mL, no remarkable changes in morphology of the fibers were observed. The hollow fibers showed an outer diameter about 800 to 1000 nm, inner diameter about 500 nm, and the thickness of the shell was about 300 to 500 nm. By increasing the concentration of PAH in core-phase solution to 15 mg/mL, the inner and outer diameter of fibers increased to about 700 and 1200 nm, respectively. Further increasing the concentration of PAH to 25 mg/mL, however, led to apparent collapse of the hollow nanofiber shell.

Influence of PAH concentration on retention efficiency of NADH in the hollow nanofibers were determined from releasing test experiments. Results in Figure 2 indicate that the nanofibers with doped PAH less than 5 mg/mL could not effectively retain NADH inside. Since the tethering of NADH to PAH was considered mainly driven by ion-exchange interactions between these two oppositely charged compounds, there would be association−dissociation equilibrium for the NADH-PAH interactions, similar to what had been found for the binding of NADPH to a positively charged surface.[29] When the PAH concentration was too low, the ionizable groups provided by PAH were not enough to provide strong NADH-PAH interactions, NADH would be dissociated from PAH and floating around. Those unbound NADH soon released into the buffer solution considering the high MWCO about 20 kDa of shell of the hollow nanofibers. Increasing the PAH concentrations from 5 to 20 mg/mL, the association of NADH to PAH was strengthened, therefore, retention efficiency of NADH higher than 95% was achieved. Further increasing PAH concentration, however, led to significant decrease in NADH retention efficiency; more than 30% of encapsulated NADH released to buffer solution once immersing the hollow nanofiber membrane into buffer. The decreased NADH retention efficiency at high PAH concentration was considered in accordance to the changes in morphology of the hollow nanofibers observed at high PAH concentration. As shown in Figure 1, at 25 and 30 mg/mL PAH concentrations, the hollow nanofibers showed a collapsed structure, probably due to too strong electrostatic repulsive force among PAH molecules doped within the shell of the hollow nanofibers. Considering the NADH retention efficiency and cost of PAH, in the following experiments, 10 mg/mL PAH was adopted for preparing hollow nanofiber for multienzyme system construction and coenzyme regeneration.

Since the retention of NADH inside the hollow nanofibers was facilitated by the ion-exchange interactions between oppositely charged NADH and PAH, changes in solution pH will possibly impose effect on the retention efficiency of NADH. We measured the surface zeta-potential of the hollow nanofibers

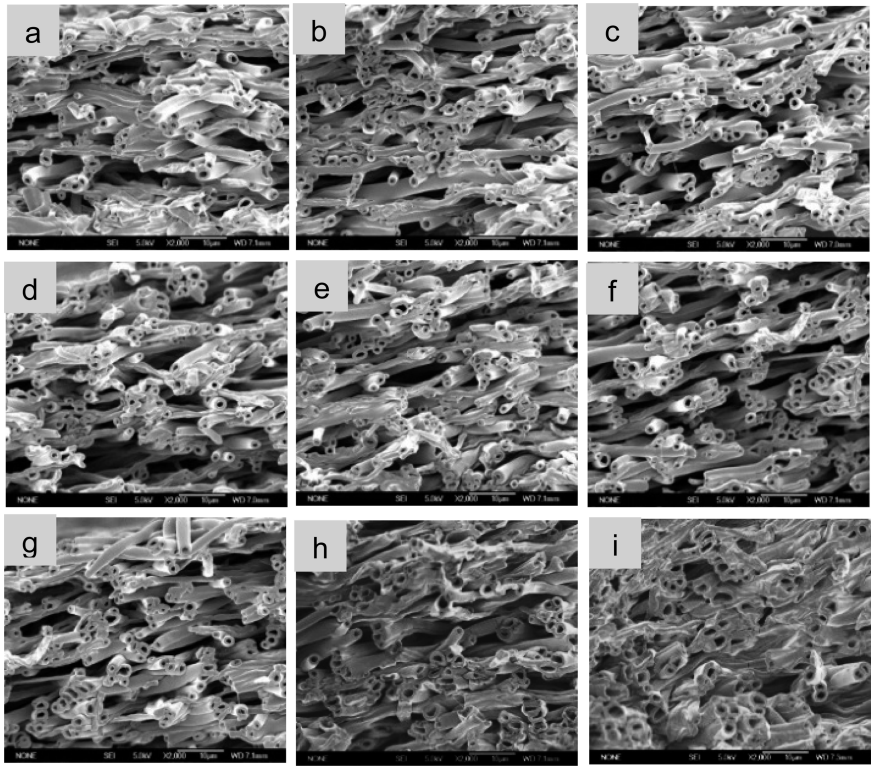

Figure 1. Cross-sectional SEM images of as-spun PAH-doped PU hollow nanofibers prepared by coaxial electrospinning with PAH concentration in core-phase solution ranging from 0 to 30 mg/mL. PAH concentrations (mg/mL): (a) 0, (b) 1.0, (c) 3.0, (d) 5.0, (e) 10.0, (f) 15.0, (g) 20.0, (h) 25.0, and (i) 30.0.

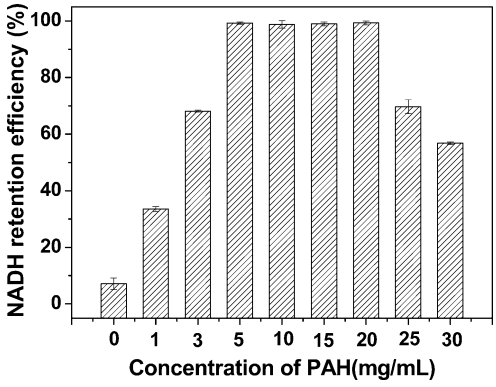

Figure 2. Influence of PAH concentration in core-phase solution for coaxial electrospinning on NADH retention efficiency in hollow nanofibers.

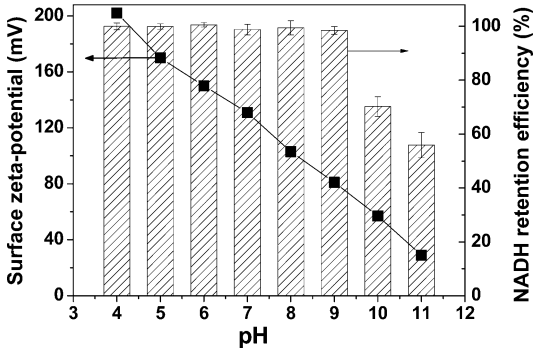

Figure 3. Influence of solution pH on the surface zeta-potential of PAH-doped PU hollow nanofibers membrane and NADH retention. The PAH-doped PU hollow nanofiber membrane was prepared by using core-phase solution containing 10 mg/mL PAH.

prepared at PAH concentration of 10 mg/mL, and then tested the NADH retention efficiency in this nanofibers by immersing the nanofibrous membrane into buffer solution of different pH. It has been reported that the PAH molecule has an isoelectric point about 13.[30] Results in Figure 3 show that on increasing solution pH over wide range from 4 to 11, surface zeta-potential of the membrane decreased approximately linearly from 202 to 29 mV. The NADH retention efficiency, however, remained almost constant until the pH increased to above 9.0, when the ion-exchange interactions between PAH and NADH became too weak to retain the NADH efficiently inside the lumen of hollow nanofibers. The stable retention of NADH over a wide range of pH, therefore, will enable us a broad range for operation in different buffer solutions.

Because of the autofluorescence property of NADH,[31,32] the retaining of NADH inside the hollow nanofibers was further confirmed by confocal laser scanning microscope (CLSM) observation. Figure 4(a) shows the bright-field CLSM image of the as-spun hollow nanofibers with encapsulated NADH, which seemed to be closely bound to the walls of the

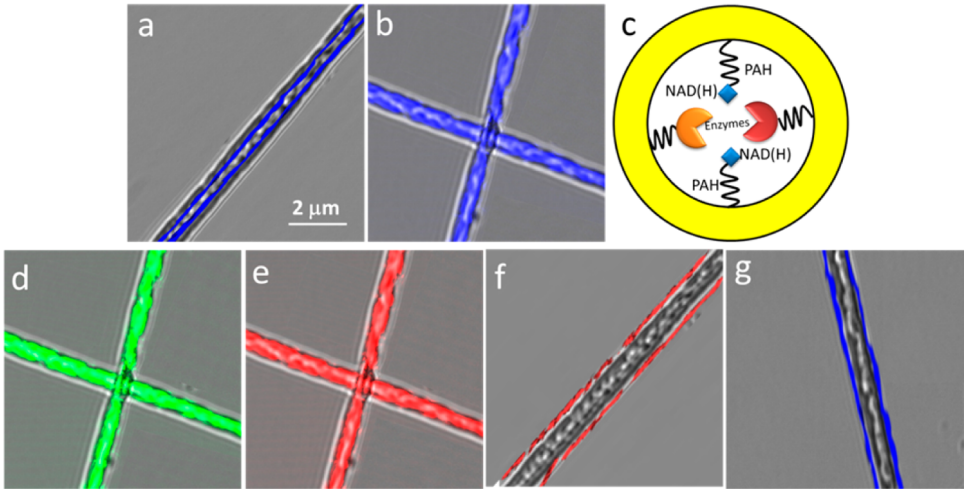

Figure 4. Confocal laser scanning microscope (CLSM) images of the PAH-doped PU hollow nanofibers with positionally assembled multienzymes and coenzymes. FateDH, FaldDH were labeled by FITC; ADH, GDH, and CA were labeled by sulforhodamine 101, respectively, prior to positional assembly. (a) The as-spun hollow nanofiber showing NADH was "glued" onto the inner wall of the fibers; (b) the hollow nanofibers after being immersed in buffer solution, showing the NADH swing freely inside the hollow chamber of nanofibers; (c) the schematic configuration of the nanostructured enzyme-cofactor-enzyme catalyst; (d) the well-distribution of FITC-labeled FateDH and FaldDH inside the lumen of the nanofibers; (e) the well-distribution of sulforhodamine 101-labeled ADH and GDH inside the lumen of the nanofibers; (f) surface attachment of CA labeled by sulforhodamine 101; (g) nanofibers with exogenous addition of NADH, showing NADH was exclusively limited to the outer surface and a thin layer of the shell of the nanofibers.

fibers; once the hollow nanofibers were immersed into buffer solution, however, almost the whole inner space of the hollow nanofibers was filled with NADH as seen from Figure 4(b). The core-phase solution for coaxial electrospinning contains 80% glycerol, which are highly viscous. During coaxial electrospinning, along with the formation of shell of the fibers by evaporating the organic solvent, glycerol in the core-phase moved to the inner wall of the shell to form the hollow chamber. During this process, the PAH tethering with NADH will be "glued" onto the inner surface of the wall along with the mobility of the glycerol.

When the hollow nanofibers membrane was immersed into buffer solution, the hollow chamber would be filled with water so that the liner PAH chain could spread out, thus allowed swing of the NADH inside the hollow chamber freely. Therefore, the PAH, which is a linear polymer with molecular weight about 200 kDa, will not only provide binding sites for efficient NADH retention, but also act as spacers to facilitate the shuttling of tethered NAD(H) between coencapsulated enzymes within the near vicinity. The thermal vibration of the active components of the catalyst system had been proven critical to the translocation of the cofactor between the two enzymes;[33] therefore, it is conceivable that further integrating of the multienzyme system inside the nanochamber of hollow nanofiber will greatly promote the coenzyme regeneration and the overall reaction kinetics. The configuration of nanostructured enzyme−cofactor−enzyme catalyst was illustrated as Figure 4(c).

Fabrication of Hollow Nanofiber-Supported Multienzyme System. The chemistry route for the synthesis of methanol from CO_2 is the same as reported previously by others,[1,16,17] which is a cascade reduction reaction catalyzed by three dehydrogenases (FateDH, FaldDH, ADH) with NADH as carrier for hydride transfer. In the present work, GDH was introduced to examine the feasibility of continuous production of methanol with *in situ* regeneration of the cofactor NADH driven by a second substrate, glutamic acid. The multienzymes and NADH were easily placed inside the lumen of the hollow nanofibers by *in situ* encapsulation during coaxial electrospinning. By using FateDH and FaldDH prelabeled with FITC, and ADH and GDH prelabeled with sulforhodamine 101 for encapsulation, the uniform dispersion of these four enzymes inside the lumen of the hollow nanofibers can be clearly seen from CLSM observations (Figure 4d and 4e). Moreover, since all these four enzymes have molecular weight larger than the MWCO of the shell of the hollow nanofibers, there was no any leakage detected by immersing the nanofiber membrane encapsulated with enzymes into buffer solution. Therefore, the amount of each of the encapsulated enzymes about 3.89 mg/g-fiber can be estimated from the concentration of the enzyme added in core-phase solution and its flow rate for coaxial electrospinning as described before.[28]

On the other hand, regarding the enzymatic reduction of CO_2, the actual reaction process is indeed more complicated since the thermodynamic equilibrium of the overall reaction is highly dependent on the solvation of CO_2. Theoretical calculation for reaction free

TABLE 1. Enzyme Loading and Activities of Multi-Enzyme System Immobilized in PAH-Doped PU Hollow Nanofibers[a]

enzyme	enzyme loading (mg/g-fiber)	activity recovery (%)	specific activity (U/mg-enzy)	gross activity (U/g-fiber)
CA	3.95 ± 0.13	66.23 ± 2.11	2.72 ± 0.09	10.75 ± 0.34
FDH	3.89 ± 0.11	63.24 ± 2.53	2.88 ± 0.11	11.19 ± 0.45
FaldDH	3.89 ± 0.14	75.95 ± 0.94	2.72 ± 0.03	10.58 ± 0.13
ADH	3.89 ± 0.05	66.79 ± 1.04	28.56 ± 0.44	111.11 ± 1.72
GDH	3.89 ± 0.08	72.79 ± 2.65	18.74 ± 0.68	72.91 ± 2.65

[a] The activities of the each enzyme were determined separately.

energy suggested the hydrated derivatives of CO_2, which involve carbonic acid (H_2CO_3), bicarbonate (HCO^{3-}), and carbonate (CO_3^{2-}), are more preferred than gaseous CO_2.[34] CA is an enzyme known to accelerate CO_2 hydration reaction with typical rate between 10^4 and 10^6 reactions per second for different forms of this enzyme.[35−39] Therefore, in an intention to accelerate the hydration reaction of CO_2 thus consequently enhance the overall CO_2 reduction reaction kinetics, CA was assembled on the outer surface of the hollow nanofiber *via* similar ion-exchange interactions between oppositely charged enzymes and the ionizable groups of PAH, which is penetrated across the shell of the hollow nanofibers. By controlling the adsorption time, a loading amount about 3.95 mg-CA/g-fiber was obtained. By labeling CA with sulforhodamine 101, its positional assembly on the outer surface of the nanofibers was also confirmed by the CLSM observation as shown in Figure 4(f).

Table 1 summarized the loading amounts and activities of each of the encapsulated enzymes (FDH, FaldDH, ADH, and GDH) and the surface-attached CA. The activities of enzymes listed in this table were individually measured using their corresponding standard substrates at well-developed measuring conditions. It can be seen that the activities recovery of all the enzymes, either encapsulated in lumen or absorbed on the outer surface of hollow nanofibers, all retained more than 60% of their activity in free formation, which can be attributed to the mild condition of immobilization process and the small mass transfer resistance due to the short diffusional distance across the shell of the hollow nanofibers.

Hollow Nanofiber-Supported Multienzyme System for Methanol Synthesis. Using the hollow nanofiber-supported system involving multienzymes and coenzyme, the methanol synthesis reaction was performed in batch mode. According to the reaction route illustrated in Scheme 1, 3 mol NADH will be consumed to produce 1 mol of methanol. Therefore, we can calculate the NADH-based methanol yield ($Y_{methanol,t}$) according to the following equation.

$$Y_{methanol,\,t}\ (\%) = \frac{3{*}C_{methanol,\,t}}{C_{NADH,\,initial}}100$$

where $C_{NADH,initial}$ was the initial NADH concentration (μM), and $C_{methanol,t}$ was the methanol concentration (μM) at time t (h).

For the hollow nanofiber-supported multienzyme system, about 50 mg of hollow nanofiber membrane was applied to the 2 mL reaction system, leading to enzyme dosage of 0.10 mg/mL for each of these five enzymes including CA, FDH, FaldDH, ADH, and GDH; dosage of NADH was 0.2 mM. At this dosage, the catalysis efficiency of free multienzyme system, however, was found too low to be able to synthesize enough methanol product for accurate concentration detection; therefore, the concentration of all these five enzymes and coenzymes were increased five times proportionally, *i.e.*, 0.50 mg/mL for CA, FDH, FaldDH, ADH, and GDH, and 1 mM for NADH.

The synthesis of methanol from CO_2 as a function of reaction time catalyzed by this five-enzyme cascade reaction was shown in Figure 5. Result was also compared with the reaction catalyzed by immobilized multienzyme systems without GDH for coenzyme regeneration and that without CA for CO_2 hydration accelerating, as well as the free multienzyme systems corresponding to each of these three combinations. Methanol yield at 10 h was calculated and depicted in Figure 5. The calculations were made on the basis of the fact that 1 mol of methanol consumes 3 mol of NADH. The free multienzyme system without coenzyme regeneration exhibited the lowest methanol yield of 27.6%. By introducing GDH and glutamate for coenzyme regeneration, the methanol yield increased to 33.1%; by further introducing CA to the reaction system for accelerating the hydration of CO_2, the methanol yield was only slightly increased to 36.2%, still far less than 100%. The potential cause for that may come from the reaction equilibria, which limits the total amount of the intermediates that can be transformed to methanol.[34]

In contrast, for all these three combinations, the methanol yields obtained by using immobilized multienzyme systems were more than 2.5-times higher than that of the corresponding free systems. Especially, for the system involving the three dehydrogenases for CO_2 reduction with coencapsulated GDH and surface-attached CA, the highest methanol yield of 103.2% was achieved, corresponding to a maximum concentration of MeOH about 68.8 μM. Since GDH was involved in the multienzyme system to regenerate NADH using glutamic acid as substrate, the methanol yield of 103.2% (exceeding 100%) suggested that the reaction thermodynamics and final equilibration of the reaction was shifted substantially toward the synthesis of methanol, and the NADH was at least partially regenerated by GDH. To the best of our knowledge, this was the highest NADH-based methanol yield which has been reported so far, and

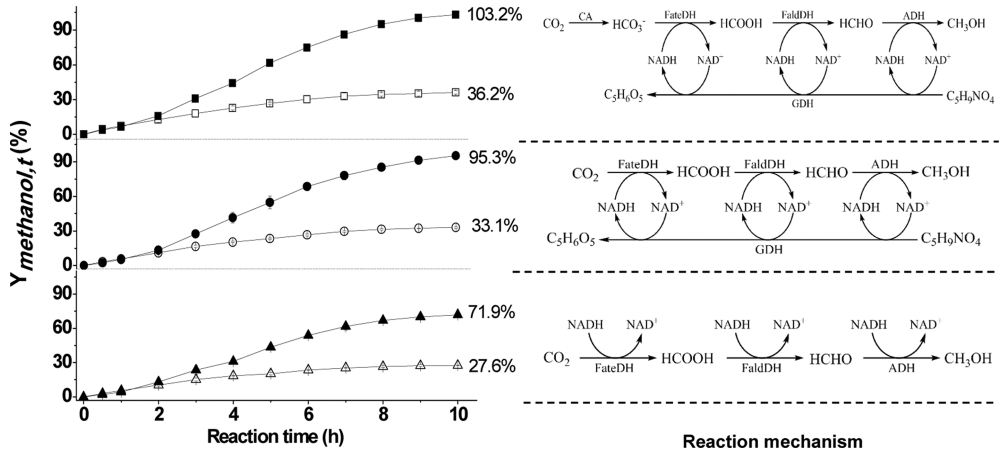

Figure 5. Plots of methanol yield as a function of reaction time for methanol synthesis from CO_2 by using multienzymes. (△, ▲) Without cofactor regeneration, (○, ●) with coupled GDH for cofactor regeneration, and (□, ■) with both GDH for cofactor regeneration and CA for accelerating hydration of CO_2. Reaction mechanisms for each multienzyme system were depicted on the right side. Open legends represent results from free multienzyme system, and the filled legends present results from the hollow nanofiber-supported multienzymes systems.

also the first time to observe the hollow-nanofiber immobilized cofactor enables reactions of immobilized multienzymes. What is more important, in most of previous studies reported by others, multienzymes were immobilized through different approaches, while cofactor were all applied in free formation, which means that reusing of expensive cofactor were impossible.[1,17−20] The only one study with immobilized enzymes and immobilized cofactor for methanol synthesis from CO_2 was based on nanoparticles, which were believed to bring the enzymes and cofactor tethered on the outer surface of nanoparticles into contact because of the collision between particles.[16] The nanoparticle-based multienzyme system, however, exhibited a methanol yield as low as only 5%, even in the presence of GDH and glutamate for cofactor regeneration.

The high methanol yield accomplished by using hollow nanofiber-supported multienzyme system in this study could be ascribed to the following aspects. First, as illustrated in Scheme 1, the utilization of CO_2 derivatives was definitely favored by introducing CA onto the outer surface of the hollow nanofiber. This was proved by the increase in methanol yield from 95.3% in the absence of CA to 103.2% in the presence of CA. The confining of the multienzymes inside the nanoscale domain of hollow nanofiber made the second contribution to the high catalytic efficiency more significant. Co-immobilizing enzymes for performing multistep biotransformations either in cascade or in coupling mode is usually kinetically advantageous over the separately immobilized system, because the second enzyme may utilize the product of the first enzyme as substrate directly at very high concentration without need of this product diffusing out from the first biocatalyst and penetrating to the second one.[40,41] With regard to the cascade reaction for CO_2 reduction, the intermediate products, including formic acid and formaldehyde, were generated and *in situ* consumed inside the nanoscale domain of hollow nanofiber without need to diffuse through long distance; the synergetic effects of multienzymes, therefore, were enhanced. Third, as illustrated by Figure 4(c) for the retention mechanism of NADH, we tend to believe that the PAH, which is a linear polymer with molecular weight of 200 kDa, not only provided tentacle points for cofactor binding *via* ion-exchange interactions, but also act as spacers to facilitate the shuttling of tethered cofactor between coencapsulated dehydrogenases within the near vicinity, thus enabling more efficient catalysis and cofactor regeneration. The feasibility of using immobilized cofactors to mediate reactions provide an easy way for cofactor recycling, which remains as the largest challenges for biotransformation involving cofactors since they are expensive and small molecules.[25,33,42−47]

TABLE 2. Methanol Production at Different Final Concentration of NADH Encapsulated Inside Lumen of Hollow Nanofibers

NADH (mM)	MeOH (μM)	$Y_{methanol,10h}$ (%)
0.05	18.44	110.64
0.1	35.79	107.37
0.2	68.78	103.17
0.3	83.54	83.54

By keeping loading amount of enzymes unchanged, while varying the NADH amount added in core-phase solution so that a final NADH concentration in reaction solution could be changed between 0.05 to 0.3 mM, we further investigated the effect of NADH concentration on the overall reaction efficiency. Results listed in Table 2 indicate that the production of

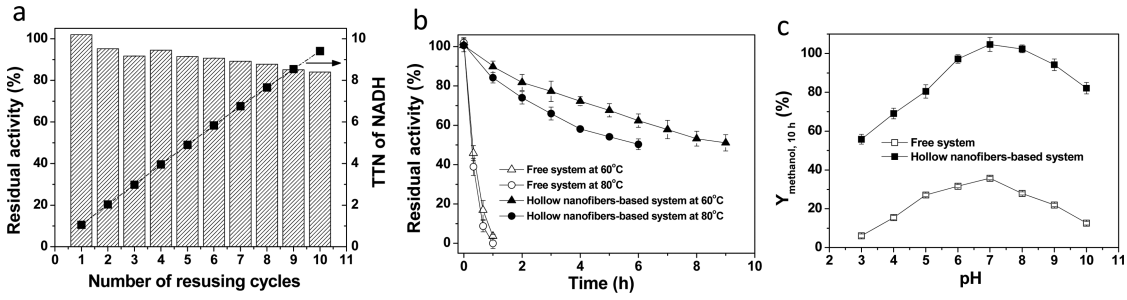

Figure 6. Performance of hollow nanofiber-supported multienzyme system for methanol synthesis from CO_2. (a) Reusability of the hollow nanofiber-supported multienzyme system and TTN of NADH, (b) thermal stability of the free and immobilized multienzyme system at 60 and 80 °C, and (c) dependence of methanol yield on pH of buffers for free and the hollow nanofiber-supported multienzyme systems.

methanol were strongly dependent on the internal cofactor concentration within the tested NADH concentration ranges. The synthesized methanol concentration after 10 h reaction increased approximately linearly until NADH concentration increase to 0.3 mM, when the $Y_{methanol,10h}$ started to decrease, indicating a superfluous of coenzyme to the enzymes.

The performance of multienzyme system trapped into the hollow fibers without involving of NADH in core solution, but exogenously added before reaction to get a final NADH concentration of 0.2 mM, was also studied. To our surprise, there was no detectable methanol synthesized even after 10 h reaction. The hollow nanofiber membrane was then picked up for CLSM observation (Figure 4g). It was found that the NADH was exclusively attached on their outer surface or entrapped into a thin layer of the hollow nanofiber shell mediated by the electrostatic interaction between NADH and PAH penetrating across the shell, thus making them inaccessible for the enzymes encapsulated inside the lumen of the hollow nanofiber. Therefore, there was no methanol synthesized. This result gives us a good demonstration of the importance of synergy between multienzymes and coenzymes.

The feasibility of recycling and reusing of the hollow nanofiber membrane-based multienzymes were examined with the system involving GDH and CA. The reaction was allowed for 6 h before they were stopped by simply retrieving the immobilized catalysts with forceps. As shown in Figure 6(a), the catalyst remained more than 80% of its original activity after 10 cycles of reusing. The 10 reusing cycles of this reaction system generated a cumulative methanol yield of 940.5%, corresponding to a total turnover number (TTN) of NADH of 9.4. Although the TTN of coenzyme was still not high enough due to reaction equilibria limit, especially since most formate dehydrogenases in nature favor the oxidation of formate, the observation of coenzyme regeneration and recycling was still exciting.

As illustrated in Figure 6(b), the immobilization of enzymes and cofactors not only realized the recycling and reusing of the biocatalysts, the nanoconfining effect of hollow nanofiber also enhanced the stability of the multienzyme system significantly. The half-life of the hollow nanofiber-based biocatalysts at 60 and 80 °C was estimated to be 6 and 9 h, respectively, which is corresponding to about 24-fold and 30-fold increase as compared with that of the free multienzymes system.

We also examined the dependence methanol yield on pH values, which theoretically will have influence on the solubility of CO_2, thus affecting the overall reaction equilibrium constants.[34−36] According to thermodynamic calculation, it was possible to shift the biological methanol metabolic reaction equilibrium constants significantly to favor the synthesis of methanol by conducting the reactions at low pHs and ionic strength.[34] Results shown in Figure 6(c), however, indicated that a neutral pH was the optimum for both the immobilized and free multienzyme systems. At pH deviated from neutral condition, the methanol yield decreased significantly. This result was mostly attributed to the effect of pH on the activity of enzymes, since FateDH, FaldDH, and ADH were all reported to have optimal pH of 7.0.[1,16,17,19]

CONCLUSION

In summary, we demonstrated that strong ion-exchange interactions between cofactor and the linear polyelectrolyte, PAH, enabled the hollow nanofiber doped with PAH as an ideal scaffold for assembly of cofactor and multienzymes. The PAH also acted as spacers for cofactor, thus increasing the flexibility of coenzyme for shuttling between different dehydrogenases. The nanoconfining effects of the hollow nanofibers afforded more efficiently synergistic catalysis and high stability for the coencapsulated multienzymes and cofactors. When the multienzyme system for methanol synthesis from CO_2 was constructed using the hollow nanofibers as a scaffold, the methanol yield of hollow nanofiber-based multienzyme system reached up to 103.17%, which was 2.85-fold higher than that of the free system. Moreover, the hollow

nanofiber-based system can be easily recovered and reused, thus improving the utilization efficiency of the catalysts for complicated bioprocessing applications.

METHODS

Materials. Formate dehydrogenase from *Candida boidinii* (FateDH, EC.1.2.1.2), formaldehyde dehydrogenase from *Pseudomonas* sp. (FaldDH, EC.1.2.1.46), yeast alcohol dehydrogenase (ADH, EC 1.1.1.1), glutamate dehydrogenase (GDH, EC.1.4.1.2), carbonic anhydrase (CA, EC.4.2.1.1), reduced cofactor nicotinamide adenine dinucleotide (NADH, 98 wt %), α-ketoglutarate, L-glutamate, poly(allylamine hydrochloride) (PAH, MW: ~200 kDa), *N*,*N*-dimethylacetylamide (DMAc), *p*-nitrophenyl acetate (*p*-NPA), *p*-nitrophenol were purchased from Sigma-Aldrich Chemical Co. (St. Louis, MO). Polyurethane A85E pellets with a bulk density of approximately 700 kg m^3 was supplied by Xiamen Jinyouju Chemical Agent Co. (Xiamen, China).

Preparation of Cationic Polyelectrolyte Doped Hollow Nanofibers for NADH Retention. General procedure for fabrication of hollow nanofibers by coaxial electrospinning: shell solution was prepared by dissolving PU in DMAc to get final polymer concentration of 25 wt %; basic core solution was a mixture solution of 200 μL of 0.1 M phosphate buffer solution (PBS, pH 7.0) and 800 μL of glycerol. The core solution and shell solution were fed at 0.07 and 0.5 mL/h, respectively, through two syringe pumps. The spinneret containing two coaxial stainless steel needles was used, with inner and outer diameters of the core nozzles used were 0.42 and 0.72 mm, and that of shell nozzle were 0.92 and 1.28 mm. A positive voltage of 20 kV was applied, and an aluminum sheet was used as the collector at a distance of 30 cm away from the nozzle tip. Electrospinning was carried out at 25 ± 3 °C, humidity 10−15%. The collected nanofiber membranes were placed overnight at room temperature to evaporate residual solvent. To prepare cationic polyelectrolyte doped hollow nanofibers suitable for NADH retention, different amount of PAH (ranges from 0 to 30 mg) and 10 mg of NADH were predissolved into the 200 μL of PBS, which was then mixed with 800 μL of glycerol to form core solution for coaxial electrospinning.

To measure the NADH retention efficiency, R_{NADH} (%), in the hollow nanofibers, the membranes collected for 30 min were immersed in 5 mL of 0.1 M PBS (pH 7.0), and incubated at 25 °C under 150 rpm shaking. At different time interval, the concentration of NADH released into buffer solution from the membrane was determined by measuring the absorbance at 340 nm, A_{340} (ε^{NADH} = 6.22 mM^{-1} cm^{-1}), using a Unico 2800 spectrophotometer. It usually takes less than 5 min to reach a constant A_{340} value in the buffer solution, indicating a release equilibrium of the encapsulated NADH. The retention efficiency, R_{NADH} (%), was then defined as the ratio of the NADH retained inside the lumen of hollow nanofiber at release equilibrium to the total amount of NADH initially encapsulated in the hollow nanofibers, which can be calculated according to the methods described in our previous study.[28]

Construction of the Hollow Nanofiber-Supported Multienzyme System. The general procedure for preparing nanofiber-supported multienzyme system for conversion of CO_2 by coaxial electrospinning was as follows: the shell solution was prepared by dissolving PU in DMAc to get a final polymer concentration of 25 wt %, the core solution was prepared by mixing 800 μL of glycerol with 200 μL of buffer solution containing 10 mg of PAH, 10 mg of FateDH, 10 mg of FaldDH, 10 mg of ADH, 14 mg of NADH, and 10 mg of GDH (for NADH regeneration). To immobilize CA on the outer surface of hollow nanofibers *via* ion-exchange interactions, 50 mg of PAH-doped PU hollow nanofibers membrane encapsulating four enzymes and NADH in hollow chamber was then immersed into PBS buffer solution (5 mL, 50 mM, pH 7.0) containing 10 mg/mL CA. The incubation was lasted for 0.5 h at 4 °C. At end of the adsorption, the nanofibers were taken out from the solution and washed several times each with 3 mL of fresh buffer until no protein was detected by Bradford method. The loading amount of CA was calculated *via* mass balance.

For comparison, the other two combinations of multienzyme system were also constructed, one of which without GDH and CA for coenzyme regeneration and for acceleration of CO_2 hydration (FateDH/FaldDH/ADH/NADH), and the other one just without involving of CA (FateDH/FaldDH/ADH/NADH/GDH). Conditions for preparing these two forms of hollow nanofiber-supported multienzyme system are the same as described above.

Activity of CA was determined by measuring the initial hydrolysis rate of *p*-NPA to *p*-nitrophenol at 25 °C. To potassium phosphate buffer solution (1 mL, 50 mM pH 7.0) containing *p*-NPA (1 mmol/L), free CA (3 μg/mL) or a piece of nanofiber membrane (about 1 mg) containing about CA (3.5 μg) were added to initiate the reaction. The reaction was monitored by measuring the absorbance at 348 nm, A_{348} ($\varepsilon^{p\text{-nitrophenol}}$ = 24.9 mM^{-1} cm^{-1}), continuously for 5 min. For the activity measurement of nanofibers enzyme, A_{348} was measured at every 30 s after retrieving the fibers with tweezers from the solution.

Activity unit of FateDH, FaldDH, and ADH were defined as the amount of enzyme needed to reduce 1 μmol formic acid, formaldehyde, or methanol, respectively, in 1 min at pH 7.0 and 25 °C. Accordingly, the activities of FateDH, FaldDH, and ADH were determined by measuring the corresponding initial reduction rate of formic acid, formaldehyde, or methanol catalyzed by each of the dehydrogenase at 25 °C, respectively. For each of the measurement, 1 mL of 50 mM pH 7.0 potassium phosphate buffer was used, concentrations of substrate (formic acid, formaldehyde, or methanol) and NADH was set as 1 and 10 mM. Free enzyme (3 μg/mL) or a piece of nanofibrous membrane (about 1 mg) containing about 3.5 μg of immobilized enzyme was added to initiate the reaction. The reaction was monitored by measuring the absorbance at 340 nm, A_{340} (ε^{NADH} =6.22 mM^{-1} cm^{-1}), continuously for 5 min. For the activity measurement of nanofibers enzyme, A_{340} was measured at every 30 s after retrieving the fibers with tweezers from the solution.

Characterization. The morphologies of the fibers were characterized by scanning electronic microscopy (SEM, JSM-6700F, JEOL, Japan). To view a cross-section of the hollow nanofibers, the collected nanofibrous membranes were frozen in liquid nitrogen, and then cut perpendicularly to the axis of the fibers, exposing their hollow structure. To determine the size distribution of the inner and outer diameters of the prepared hollow PU nanofibers, approximately 100 nanofibers were analyzed from the SEM images.

In order to characterize the distribution of enzymes and NADH, which are positionally assembled in polyelectrolyte doped hollow nanofibers, FateDH and FaldDH were labeled by FITC, while ADH, GDH, and CA were labeled by sulforhodamine 101 prior to positional assembly. The hollow nanofibers with positional assembled enzymes were then characterized by confocal laser scanning microscopy (CLSM) with Leica TCS SP5 microscope (Leica Camera AG, Germany). The laser provided excitation of FITC and sulforhodamine 101 at 488 and 586 nm, and emitted fluorescent light was detected at 545 and 605 nm, respectively. Because of the autofluorescence of NADH,[31,32] the laser provided excitation of NADH at 351 nm, and emitted fluorescent light was detected at 460 nm.

To detect the possible leakage of encapsulated enzymes, about 100 mg of hollow nanofibers membrane encapsulating four enzymes and NADH in hollow chamber was immersed into PBS buffer solution (5 mL, 50 mM, pH 7.0), and the protein concentration in buffer solution were assayed by Bradford method.

Enzymatic Synthesis of Methanol from CO_2. CO_2 was converted into methanol by conducting reduction reactions in aqueous solution with free or immobilized multienzymes. The experimental setup used in this study was described in detail in

Scheme 1. Synthesis of methanol by the free and immobilized multienzyme system were performed as follows. Briefly, 2 mL of buffer solution (50 mM PBS, pH 7.0) containing 10 mM L-glutamate was bubbled with CO_2 gas for 0.5 h, and then 50 mg of hollow nanofiber membrane-based multienzyme system was added to initiate the reaction. When free multienzyme system was used, 2 mL of the buffer solution containing 10 mM L-glutamate and the five enzymes (CA, FateDH, FaldDH, ADH, and GDH) was bubbled with CO_2 gas for 0.5 h. Dosage of each enzyme was 0.5 mg/mL. The reaction was initiated by adding NADH to the reactant to get a concentration of 1 mM. For both immobilized and free multienzyme system, the pressure was maintained at 0.3 MPa by regulating the counterbalance valve, and no outward gas flow was permitted during the reaction to avoid the evaporating of synthesized methanol. At time intervals, 20 μL of sample was taken from the reaction mixture for methanol concentration measurement after pressure release.

A gas chromatography (Agilent 7890A) equipped with a flame ionization detector (FID) and an Agilent HP-FFAP gas column (25 m $\times$ 0.320 mm $\times$ 0.50 μm) was used for the analysis of methanol concentration. The initial column temperature was kept at 75 °C for 10 min. The injector and detector temperatures were 150 and 300 °C, respectively. Nitrogen was used as the carrier gas at an inlet pressure of 18 kPa ($\sim$0.4 mL/min). The injection volume was 1 μL.

Enzyme Stability Tests. Reusability of the immobilized multienzyme system was examined by measuring the methanol yield during repeated usages. The reactions lasted for 6 h before they were stopped by retrieving the immobilized catalysts with a forceps. After washing the hollow nanofiber-supported multienzyme system with buffer solution, fresh substrates were added, and the next reaction measurement was carried out. The time interval between one reaction cycle to the next round was about 1 h. The methanol yield of the freshly prepared multienzymes system was defined as 100%.

The stabilities of the multienzyme system was examined by monitoring changes in methanol yield ($Y_{methanol,10h}$) after 10 h reaction as a function of incubation time under specific conditions. Native multienzyme system was dissolved in potassium phosphate buffer solutions (50 mM pH 7.0) and stored in an incubator with the temperature controlled at 60 or 80 °C. Hollow nanofiber-supported multienzyme system was sealed in plastic Ziploc bags, and stored in the incubator with the temperature controlled in the range of 60 to 80 °C. The residual activity of the multienzyme system was measured periodically.

Conflict of Interest: The authors declare no competing financial interest.

Acknowledgment. The authors are thankful for support from the National Natural Science Foundation of China (Grant Nos. 21376249, 21336010, 20976180), and the National Basic Research Program of China (973 Program, 2013CB733604).

REFERENCES AND NOTES

1. Obert, R.; Dave, B. C. Enzymatic Conversion of Carbon Dioxide to Methanol: Enhanced Methanol Production in Silica Sol−Gel Matrices. *J. Am. Chem. Soc.* **1999**, *121*, 12192–12193.
2. Appel, A. M.; Bercaw, J. E.; Bocarsly, A. B.; Dobbek, H.; DuBois, D. L.; Dupuis, M.; Ferry, J. G.; Fujita, E.; Hille, R.; Kenis, P. J.; *et al.* Opportunities, and Challenges in Biochemical and Chemical Catalysis of CO_2 Fixation. *Chem. Rev.* **2013**, *113*, 6621–6658.
3. Hawkins, A. S.; McTernan, P. M.; Lian, H.; Kelly, R. M.; Adams, M. W. Biological Conversion of Carbon Dioxide and Hydrogen into Liquid Fuels and Industrial Chemicals. *Curr. Opin. Biotechnol.* **2013**, *24*, 376–384.
4. Mikkelsen, M.; Jørgensen, M.; Krebs, F. C. The Teraton Challenge. A Review of Fixation and Transformation of Carbon Dioxide. *Energy Environ. Sci.* **2010**, *3*, 43–81.
5. Ibrahim, N.; Kamarudin, S. K.; Minggu, L. J. Biofuel from Biomass *via* Photo-Electrochemical Reactions: An Overview. *J. Power Sources* **2014**, *259*, 33–42.
6. Ohta, K.; Kawamoto, M.; Mizuno, T.; Lowy, D. A. Electrochemical Reduction of Carbon Dioxide in Methanol at Ambient Temperature and Pressure. *J. Appl. Electrochem.* **1998**, *28*, 717–724.
7. You, E.; Guzmán-Blas, R.; Nicolau, E.; Aulice Scibioh, M.; Karanikas, C. F.; Watkins, J. J.; Cabrera, C. R. Co-Deposition of Pt and Ceria Anode Catalyst in Supercritical Carbon Dioxide for Direct Methanol Fuel Cell Applications. *Electrochim. Acta* **2012**, *75*, 191–200.
8. Kuwabata, S.; Tsuda, R.; Yoneyama, H. Electrochemical Conversion of Carbon Dioxide to Methanol with the Assistance of Formate Dehydrogenase and Methanol Dehydrogenase as Biocatalysts. *J. Am. Chem. Soc.* **1994**, *116*, 5437–5443.
9. Olah, G. A.; Goeppert, A.; Prakash, G. K. S. Chemical Recycling of Carbon Dioxide to Methanol and Dimethyl Ether: from Greenhouse Gas to Renewable, Environmentally Carbon Neutral Fuels and Synthetic Hydrocarbons. *J. Org. Chem.* **2008**, *74*, 487–498.
10. Qiao, J.; Liu, Y.; Hong, F.; Zhang, J. A Review of Catalysts for the Electroreduction of Carbon Dioxide to Produce Low-Carbon Fuels. *Chem. Soc. Rev.* **2014**, *43*, 631–675.
11. Ganesh, I. Conversion of Carbon Dioxide into Methanol—A Potential Liquid Fuel: Fundamental Challenges and Opportunities (A Review). *Renewable Sustainable Energy Rev.* **2014**, *31*, 221–257.
12. Boston, D. J.; Xu, C.; Armstrong, D. W.; MacDonnell, F. M. Photochemical Reduction of Carbon Dioxide to Methanol and Formate in A Homogeneous System with Pyridinium Catalysts. *J. Am. Chem. Soc.* **2013**, *135*, 16252–16255.
13. Amao, Y.; Watanabe, T. Photochemical and Enzymatic Methanol Synthesis from HCO_3^- by Dehydrogenases Using Water-Soluble Zinc Porphyrin in Aqueous Media. *Appl. Catal., B* **2009**, *86*, 109–113.
14. Tan, S. S.; Zou, L.; Hu, E. Photocatalytic Reduction of Carbon Dioxide into Gaseous Hydrocarbon Using TiO_2 Pellets. *Catal. Today* **2006**, *115*, 269–273.
15. Cazelles, R.; Drone, J.; Fajula, F.; Ersen, O.; Moldovan, S.; Galarneau, A. Reduction of CO_2 to Methanol by A Polyenzymatic System Encapsulated in Phospholipids−Silica Nanocapsules. *New J. Chem.* **2013**, *37*, 3721–3730.
16. El-Zahab, B.; Donnelly, D.; Wang, P. Particle-Tethered NADH for Production of Methanol from CO_2 Catalyzed by Coimmobilized Enzymes. *Biotechnol. Bioeng.* **2008**, *99*, 508–514.
17. Wang, X.; Li, Z.; Shi, J.; Wu, H.; Jiang, Z.; Zhang, W.; Song, X.; Ai, Q. Bioinspired Approach to Multienzyme Cascade System Construction for Efficient Carbon Dioxide Reduction. *ACS Catal.* **2014**, *4*, 962–972.
18. Sun, Q.; Jiang, Y.; Jiang, Z.; Zhang, L.; Sun, X.; Li, J. Green and Efficient Conversion of CO_2 to Methanol by Biomimetic Coimmobilization of Three Dehydrogenases in Protamine-Templated Titania. *Ind. Eng. Chem. Res.* **2009**, *48*, 4210–4215.
19. Xu, S. W.; Lu, Y.; Li, J.; Jiang, Z. Y.; Wu, H. Efficient Conversion of CO_2 to Methanol Catalyzed by Three Dehydrogenases Co-Encapsulated in An Alginate−Silica (ALG−SiO_2) Hybrid Gel. *Ind. Eng. Chem. Res.* **2006**, *45*, 4567–4573.
20. Jiang, Y. J.; Sun, Q. Y.; Zhang, L.; Jiang, Z. Y. Capsules-in-Bead Scaffold: A Rational Architecture for Spatially Separated Multienzyme Cascade System. *J. Mater. Chem.* **2009**, *19*, 9068–9074.
21. Forsyth, C.; Yip, T. W.; Patwardhan, S. V. CO_2 Sequestration by Enzyme Immobilized onto Bioinspired Silica. *Chem. Commun.* **2013**, *49*, 3191–3193.
22. Glueck, S. M.; Gumus, S.; Fabian, W. M.; Faber, K. Biocatalytic Carboxylation. *Chem. Soc. Rev.* **2010**, *39*, 313–328.
23. Aresta, M.; Dibenedetto, A.; Baran, T.; Angelini, A.; Łabuz, P.; Macyk, W. An Integrated Photocatalytic/Enzymatic System for the Reduction of CO_2 to Methanol in Bioglycerol−Water. *Beilstein J. Org. Chem.* **2014**, *10*, 2556–2565.
24. Jia, H.; Zhu, G.; Wang, P. Catalytic Behaviors of Enzymes Attached to Nanoparticles: the Effect of Particle Mobility. *Biotechnol. Bioeng.* **2003**, *84*, 406–414.

25. Zheng, M.; Zhang, S.; Ma, G.; Wang, P. Effect of Molecular Mobility on Coupled Enzymatic Reactions Involving Cofactor Regeneration Using Nanoparticle-Attached Enzymes. *J. Biotechnol.* **2011**, *154*, 274–280.
26. Zheng, M.; Su, Z.; Ji, X.; Ma, G.; Wang, P.; Zhang, S. Magnetic Field Intensified Bi-Enzyme System with *in situ* Cofactor Regeneration Supported by Magnetic Nanoparticles. *J. Biotechnol.* **2013**, *168*, 212–7.
27. Fu, J.; Yang, Y. R.; Johnson-Buck, A.; Liu, M.; Liu, Y.; Walter, N. G.; Woodbury, N. W.; Yan, H. Multi-Enzyme Complexes on DNA Scaffolds Capable of Substrate Channelling with An Artificial Swinging Arm. *Nat. Nanotechnol.* **2014**, *9*, 531–536.
28. Ji, X.; Wang, P.; Su, Z.; Ma, G.; Zhang, S. Enabling Multi-Enzyme Biocatalysis Using Coaxial-Electrospun Hollow Nanofibers: Redesign of Artificial Cells. *J. Mater. Chem. B* **2014**, *2*, 181.
29. da Silva, E. S.; Gómez-Vallejo, V.; Llop, J.; López-Gallego, F. Efficient Nitrogen-13 Radiochemistry Catalyzed by A Highly Stable Immobilized Biocatalyst. *Catal. Sci. Technol.* **2015**, 10.1039/c5cy00179j.
30. Ji, X.; Su, Z.; Wang, P.; Ma, G.; Zhang, S. Polyelectrolyte Doped Hollow Nanofibers for Positional Assembly of Bienzyme System for Cascade Reaction at O/W Interface. *ACS Catal.* **2014**, *4*, 4548–4559.
31. Barlow, C.; Chance, B. Ischemic Areas in Perfused Rat Hearts: Measurement by NADH Fluorescence Photography. *Science* **1976**, *193*, 909–910.
32. Mayevsky, A.; Rogatsky, G. G. Mitochondrial Function *in vivo* Evaluated by NADH Fluorescence: from Animal Models to Human Studies. *Am. J. Physiol. Cell Physiol.* **2007**, *292*, 615–640.
33. El-Zahab, B.; Jia, H.; Wang, P. Enabling Multienzyme Biocatalysis Using Nanoporous Materials. *Biotechnol. Bioeng.* **2004**, *87*, 178–183.
34. Baskaya, F. S.; Zhao, X.; Flickinger, M. C.; Wang, P. Thermodynamic Feasibility of Enzymatic Reduction of Carbon Dioxide to Methanol. *Appl. Biochem. Biotechnol.* **2010**, *162*, 391–398.
35. Favre, N.; Christ, M. L.; Pierre, A. C. Biocatalytic Capture of CO_2 with Carbonic Anhydrase and Its Transformation to Solid Carbonate. *J. Mol. Catal. B: Enzym.* **2009**, *60*, 163–170.
36. Favre, N.; Ahmad, Y.; Pierre, A. Biomaterials Obtained by Gelation of Silica Precursor with CO_2 Saturated Water Containing A Carbonic Anhydrase Enzyme. *J. Sol-Gel Sci. Technol.* **2011**, *58*, 442–451.
37. Sharma, A.; Bhattacharya, A. Enhanced Biomimetic Sequestration of CO_2 into $CaCO_3$ Using Purified Carbonic Anhydrase from Indigenous Bacterial Strains. *J. Mol. Catal. B: Enzym.* **2010**, *67*, 122–128.
38. Patel, T. N.; Park, A.-H. A.; Banta, S. Periplasmic Expression of Carbonic Anhydrase in *Escherichia coli*: A New Biocatalyst for CO_2 Hydration. *Biotechnol. Bioeng.* **2013**, *110*, 1865–1873.
39. Smith, K. S.; Ferry, J. G. Prokaryotic Carbonic Anhydrases. *FEMS Microbiol. Rev.* **2000**, *24*, 335–366.
40. Rocha-Martín, J.; Rivas, B. d. l.; Muñoz, R.; Guisán, J. M.; López-Gallego, F. Rational Co-immobilization of Bi-Enzyme Cascades on Porous Supports and Their Applications in Bio-redox Reactions with *in situ* Recycling of Soluble Cofactors. *ChemCatChem* **2012**, *4*, 1279–1288.
41. Garcia-Galan, C.; Berenguer-Murcia, Á.; Fernandez-Lafuente, R.; Rodrigues, R. C. Potential of Different Enzyme Immobilization Strategies to Improve Enzyme Performance. *Adv. Synth. Catal.* **2011**, *353*, 2885–2904.
42. Gu, K. F.; Chang, T. M. S. Production of Essential L-Branched-Chain Amino Acids in Bioreactors Containing Artificial Cells Immobilized Multienzyme Systems and Dextran-NAD^+. *Biotechnol. Bioeng.* **1990**, *36*, 263–269.
43. Persson, M.; Mansson, M.-O.; Bulow, L.; Mosbach, K. Continuous Regeneration of NAD(H) Covalently Bound to a Cysteine Genetically Engineered into Glucose Dehydrogenase. *Nat. Biotechnol.* **1991**, *9*, 280–284.
44. Obón, J.; Almagro, M. J.; Manjón, A.; Iborra, J. Continuous Retention of Native NADP(H) in An Enzyme Membrane Reactor for Gluconate and Glutamate Production. *J. Biotechnol.* **1996**, *50*, 27–36.
45. Obón, J. M.; Manjón, A.; Iborra, J. L. Retention and Regeneration of Native NAD(H) in Noncharged Ultrafiltration Membrane Reactors: Application to L-lactate and Gluconate Production. *Biotechnol. Bioeng.* **1998**, *57*, 510–517.
46. Lin, S. S.; Miyawaki, O.; Nakamura, K. Continuous Production of L-carnitine with NADH Regeneration by A Nanofiltration Membrane Reactor with Coimmobilized L-carnitine Dehydrogenase and Glucose Dehydrogenase. *J. Biosci. Bioeng.* **1999**, *87*, 361–364.
47. Zhang, Y.; Gao, F.; Zhang, S. P.; Su, Z. G.; Ma, G. H.; Wang, P. Simultaneous Production of 1,3-Dihydroxyacetone and Xylitol from Glycerol and Xylose Using A Nanoparticle-Supported Multi-Enzyme System with *in situ* Cofactor Regeneration. *Bioresour. Technol.* **2011**, *102*, 1837–43.